



## CHARACTERIZATION OF NEUTRON FLUX IN THE EXPOSURE CHANNEL F19 OF THE TRIGA MARK II REACTOR IN LJUBLJANA

Edvard S. Krištof

Institut Jožef Stefan, Jamova 39, Ljubljana, Slovenia

### Abstract

In this paper a description of the neutron flux in the vertical irradiation channel F19 of the Ljubljana TRIGA reactor is given. In this channel small samples of materials that are well known in reactor metrology such as gold, indium, aluminium, etc. were irradiated. After irradiations gamma ray spectra were measured and from the saturation activities of suitable reactions the neutron spectrum was calculated. Also, the variation of the thermal flux around the circumference of the container was determined.

### Introduction

The channel F19 is one of the most used irradiation facilities of our reactor. For example, in the last two years irradiations of minerals with the aim of determining their age, and many semiconductor materials for studying changes in their properties due to fast neutron bombardment were carried out. Anyhow, for an evaluation of data the neutron flux spectrum must be known. For this reason the  $^{197}\text{Au}(n,\gamma)$  reaction with bare diluted gold,  $^{197}\text{Au}(n,\gamma)$  with diluted gold under cadmium cover,  $^{115}\text{In}(n,\gamma)$  with diluted indium under cadmium cover,  $^{58}\text{Fe}(n,\gamma)$  under cadmium cover,  $^{63}\text{Cu}(n,\gamma)$ ,  $^{63}\text{Cu}(n,\gamma)$  under cadmium cover and the threshold reactions  $^{115}\text{In}(n,n')$ ,  $^{27}\text{Al}(n,\alpha)$ ,  $^{59}\text{Co}(n,\alpha)$ ,  $^{59}\text{Co}(n,p)$  were utilized.

### Irradiation set-up

A simplified cross-section through the reactor core at the half height of the fuel elements is shown in Fig. 1. Letters OK, CK and PP denote vertical irradiation channels.

A sample for irradiation is put in a cylindrical container of aluminium. The outer diameter of the container is 2.5cm, and its usable height is 8cm. Irradiation of the sample begins by lowering the container into the core, and finishes by lifting it back, or by scrambling the reactor.

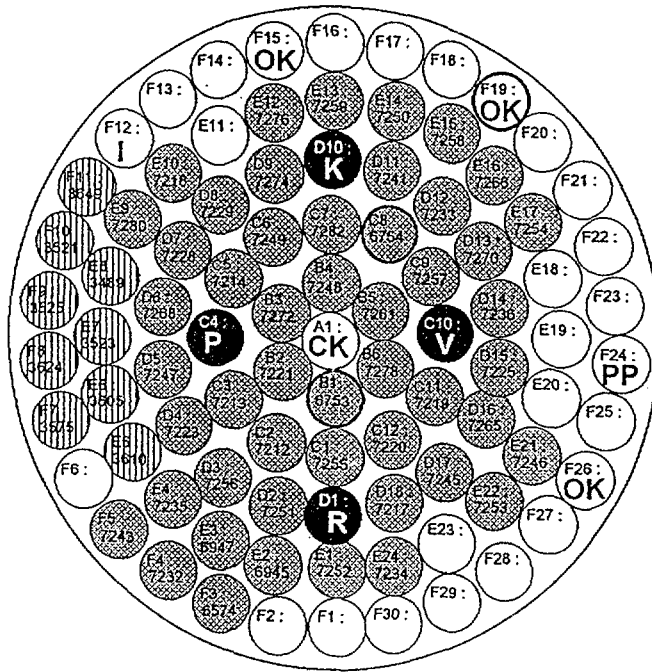


**Figure 1:** Simplified cross-section through the reactor core at the half height of the fuel elements. Letters OK, CK and PP denote vertical irradiation channels. Black circles are control rods, hatched circles are graphite elements and shadowed ones are fuel elements.

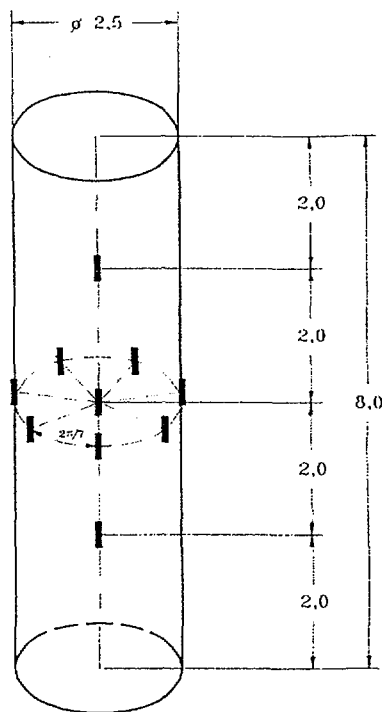


**Figure 2:** Position of small wires of diluted gold around the circumference of the aluminium container and on its axis.

## Irradiations and ancillary measurements

All irradiations were performed at full reactor power of 250 kW. The samples were fixed in the axis of the container 4cm from the bottom. Each irradiation was monitored by a small wire with bare diluted gold, which was mounted on the axis 2cm from the bottom. After irradiation of the activation materials, suitable  $\gamma$ -spectrometric measurements were carried out. The data, which are necessary to evaluate these measurements, were taken from the literature [2–5].

Because some users of the channel F19 monitored their irradiations by mounting the detection material on the outer surface of the container, an additional irradiation was performed to estimate the error due to variation of the slow neutron flux around the circumference of the container. In this case only bare diluted gold was used. Small wires were fixed on the outer surface of the container 4cm from the bottom in steps of  $2\pi/7$ , and a further three were on the axis at heights of 2cm, 4cm, 6cm (see Fig.2).

## Results

From the measured saturation activities the neutron flux spectrum was determined (see Fig.3) by use of the computer package SAND II [1]. The total flux at 250 kW was

$$\Phi_{total} = \int_0^{20\text{MeV}} \phi(E) dE = 6.54(1 \pm 0.015) \cdot 10^{12} \text{ cm}^{-2} \text{ s}^{-1}$$

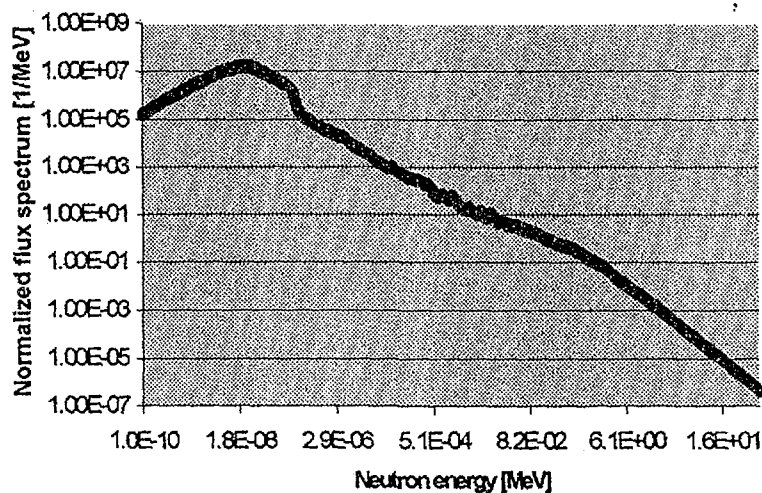


Figure 3: Normalized neutron flux spectrum  $\psi(E) = \Phi(E) / \text{const}$ ,

where  $\text{const} = 1.817 \cdot 10^{12} \text{ cm}^{-2} \text{ s}^{-1}$ , so that  $\int_{100\text{keV}}^{20\text{MeV}} \Psi(E) dE = 1$

Integrals of the neutron spectrum at the most characteristic regions are

$$\Phi_{thermal} = \int_0^{0.5eV} \phi(E) dE = 3.19(1 \pm 0.029) \cdot 10^{12} \text{ cm}^{-2} \text{ s}^{-1}$$

$$\Phi_{intermediate} = \int_{0.5eV}^{100keV} \phi(E) dE = 1.53(1 \pm 0.021) \cdot 10^{12} \text{ cm}^{-2} \text{ s}^{-1}$$

$$\Phi_{fast} = \int_{100keV}^{20MeV} \phi(E) dE = 1.82(1 \pm 0.024) \cdot 10^{12} \text{ cm}^{-2} \text{ s}^{-1}$$

The error in these values was determined with variation of the saturation activities considering the uncertainties of all the individual  $\gamma$ -spectrometric measurements.

The saturation activity for the reaction  $^{197}\text{Au}(n,\gamma)$  at discrete values of the azimuthal angle  $\vartheta$  is given in the Table 1. The Fourier trigonometric sum  $S_3 = a(\vartheta)$  with the property  $a(\vartheta_i) = a_i$  is shown in the Fig. 4. The ratio  $a_{max}/a_{min}$  between the extreme values is equal to 1.10. The average value of  $a(\vartheta)$  is

$$\bar{a} = \frac{\int_0^{2\pi} a(\vartheta) d\vartheta}{2\pi} = \frac{\sum_{i=1}^7 a_i}{7} = 0.5066 \cdot 10^{-9} \frac{\text{Bq}}{\text{nucleus } ^{197}\text{Au}}$$

The number

$$\varepsilon = \frac{\sqrt{\int_0^{2\pi} (a(\vartheta) - \bar{a})^2 d\vartheta}}{\bar{a} \sqrt{2\pi}} = 0.030$$

is significant. Namely, the average value  $\bar{a}$  coincides with the value  $a_9$  in the centre at  $R=0$ ,  $H=4\text{cm}$  within its error. So  $\varepsilon$  is the expected systematic error for a single irradiation whenever the fluence is monitored on the surface of the container. This error must be added to errors of other origin.

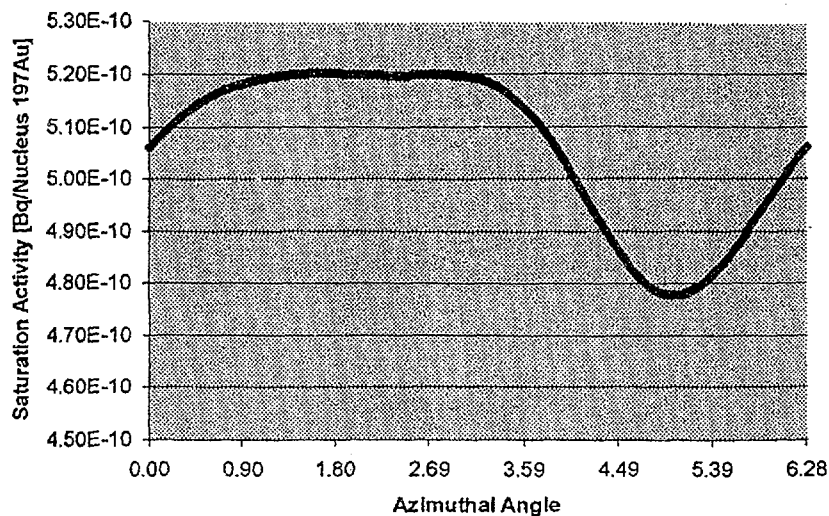


Figure 4:  $^{197}\text{Au}(n, \gamma)$  saturation activity on the circumference of the container as function of azimuthal angle  $\vartheta$

Table 1:  $^{197}\text{Au}(n, \gamma)$  saturation activity of small wires. Counting errors are given in parentheses.

i	azimuthal angle $\vartheta_i$	R	H	saturation activity Bq/nucle. $^{197}\text{Au}$
1	0	1.30cm	4cm	$0.5143 \cdot 10^{-9}$ ( $1 \pm 0.008$ )
2	$2\pi/7$	1.30cm	4cm	$0.5200 \cdot 10^{-9}$ ( $1 \pm 0.009$ )
3	$4\pi/7$	1.30cm	4cm	$0.5200 \cdot 10^{-9}$ ( $1 \pm 0.008$ )
4	$6\pi/7$	1.30cm	4cm	$0.5193 \cdot 10^{-9}$ ( $1 \pm 0.009$ )
5	$8\pi/7$	1.30cm	4cm	$0.5014 \cdot 10^{-9}$ ( $1 \pm 0.010$ )
6	$10\pi/7$	1.30cm	4cm	$0.4781 \cdot 10^{-9}$ ( $1 \pm 0.009$ )
7	$12\pi/7$	1.30cm	4cm	$0.4934 \cdot 10^{-9}$ ( $1 \pm 0.010$ )
8	/	0	2cm	$0.5128 \cdot 10^{-9}$ ( $1 \pm 0.008$ )
9	/	0	4cm	$0.5030 \cdot 10^{-9}$ ( $1 \pm 0.008$ )
10	/	0	6cm	$0.4956 \cdot 10^{-9}$ ( $1 \pm 0.007$ )

## Acknowledgement

*I would like to thank Bojan Huzjan, Janez Jezeršek, Darko Kavšek, Mitja Kožuh, Bojan Oman, Gvido Pregl and Marko Rosman for kind support, and Jože Rant for obtaining the software package SAND II.*

## References

- [1] SAND II - Neutron Flux Spectra Determination by Multiple Foil Activation, January 1994, Oak Ridge National Laboratory, USA.
- [2] J. H. Baard, W. L. Zijp, H. J. Nolthenius,  
Nuclear Data Guide for Reactor Neutron Metrology, Kluwer Academic Publishers, 1989,  
Dordrecht, The Netherlands.
- [3] JEF-PC, A personal Computer Program for Displaying Nuclear Data from the Joint  
Evaluated File Library, 1997, OECD Nuclear Energy Agency, Issy-les-Moulineaux, France.
- [4] N. G. Gusev and P. P. Dmitriev,  
Quantum Radiation of Radioactive Nuclides, 1979, Pergamon Press, Kronberg – Taunus,  
Germany
- [5] W. Seelman-Eggelbert et al, Karlsruher Nuklidkarte, Kernforschungszentrum, Karlsruhe,  
Germany.